ADVANCING EARTH AND SPACE SCIENCE

Geophysical Research Letters

RESEARCH LETTER
10.1029/2022GL099794

Special Section:
Results from Juno's Flyby of Ganymede

Key Points:
- The high spatial resolution observations revealed auroral emissions of over 1000 Rayleighs, brighter than previously observed
- The leading hemisphere aurora exhibits an intense auroral curtain with a sharp poleward boundary and more slowly tapering equatorial edge
- Juno-UVS observed Ganymede's auroral emissions extending up to a maximum of 50 km altitude

Supporting Information:

Supporting Information may be found in the online version of this article.

Correspondence to:

T. K. Greathouse,
tgreathouse@swri.edu

Citation:

Greathouse, T. K., Gladstone, G. R., Molyneux, P. M., Versteeg, M. H., Hue, V., Kammer, J. A., et al. (2022). UVS observations of Ganymede's aurora during Juno orbits 34 and 35. *Geophysical Research Letters*, *49*, e2022GL099794. https://doi.org/10.1029/2022GL099794

Received 3 JUN 2022
Accepted 31 OCT 2022

UVS Observations of Ganymede's Aurora During Juno Orbits 34 and 35

T. K. Greathouse[1], G. R. Gladstone[1,2], P. M. Molyneux[1], M. H. Versteeg[1], V. Hue[1], J. A. Kammer[1], M. W. Davis[1], S. J. Bolton[1], R. S. Giles[1], J. E. P. Connerney[3,4], J.-C. Gerard[5], D. C. Grodent[5], B. Bonfond[5], J. Saur[6], and S. Duling[6]

[1]Southwest Research Institute, San Antonio, TX, USA, [2]University of Texas at San Antonio, San Antonio, TX, USA, [3]NASA Goddard Space Flight Center, Greenbelt, MD, USA, [4]Space Research Corporation, Annapolis, MD, USA, [5]Université de Liège, LPAP – STAR Institute, Liège, Belgium, [6]University of Cologne, Cologne, Germany

Abstract On 7 June 2021, Juno-UVS mapped Ganymede's auroral emissions near a closest approach altitude of 1,046 km. The high spatial resolution map exhibits bright, 200–1,000 R, oxygen emissions organized into northern and southern auroral ovals. Though the map has incomplete global coverage, UVS observed longitudinal structure similar to that described by McGrath et al. (2013), https://doi.org/10.1002/jgra.50122 and latitudinal and vertical structure never before resolved. The mapped auroral emissions (a) display an intense narrow auroral curtain with a sharp poleward boundary, (b) have a more slowly decreasing equatorial edge on the leading hemisphere, (c) appear to originate near the surface with a vertical extent of 25–50 km, and (d) are slightly brighter in the north than the south. Additionally, we present UVS observations from the more distant Juno Ganymede flyby on 20 July 2021. We describe the observations, compare them to previous Hubble Space Telescope observations and current model predictions of the open-closed-field line-boundary.

Plain Language Summary Observations of Ganymede by Juno-UVS during a close flyby (during Juno's 34th Jupiter orbit) captured unique high-spatial-resolution measurements of Ganymede's auroral emissions. Organized into two polar ovals, the positions and intensities of the auroral emissions are consistent with previous Hubble Space Telescope observations. The observed morphology of the auroras on the leading hemisphere of Ganymede exhibits latitudinal structure never before resolved. Previous studies suggest the poleward edge of the emissions trace the poleward most position of the magnetic field lines that have both ends rooted to Ganymede. We show that a magnetic field model of Ganymede within Jupiter's larger magnetosphere predicts last-closed field-lines very close to the observed auroral emissions, as expected. More distant observations taken during Juno's following orbit (orbit 35) capture auroral emissions at slightly different longitudes. They too show similar agreement with previous observations and current magnetic field models.

1. Introduction

During the Galileo mission in June and July of 1996 Hall et al. (1998), using the Hubble Space Telescope (HST) Goddard High Resolution Spectrograph, captured the first UV measurements of the 130.4 and 135.6 nm oxygen emission lines from Ganymede. The flux ratio of the 135.6/130.4 emission (~1 to 2) suggested the emissions were produced by electron impact excitation of an O_2-dominated atmosphere. The observed spatial variation along the slit, taken in concert with the Galileo magnetometer (Kivelson et al., 1996) and plasma wave (Gurnett et al., 1996) measurements, suggested that the emissions were likely from northern and southern auroral ovals (Hall et al., 1998).

Since that time, Feldman et al. (2000) performed observations of Ganymede's trailing hemisphere using the Space Telescope Imaging Spectrograph (STIS) on HST, and showed that the auroral emissions were both temporally and spatially variable.

Adding several more HST/STIS observations of Ganymede to the collection, uniquely of the leading and sub-Jovian hemispheres, along with an observation taken with the Advanced Camera for Surveys, also on HST, McGrath et al. (2013) confirmed the temporal variability seen by Feldman et al. (2000) and discovered that the auroral ovals were located at high latitude on Ganymede's trailing hemisphere (the hemisphere being impacted by Jupiter's corotating plasma) and lower latitude on Ganymede's leading hemisphere. Eviatar et al. (2001) showed that the energy of the Jovian corotating plasma was insufficient to excite such auroral emissions alone suggesting

10.1029/2022GL099794

that the electrons responsible for the auroral emissions must be accelerated, possibly in the reconnection region between Ganymede's and Jupiter's magnetospheres. Plasma interaction modeling of Ganymede's magnetosphere suggested that the auroras would occur near the boundary between open- and closed-magnetic field-lines, providing valuable information about the structure and evolution of Ganymede's magnetic field (Saur et al., 2015), as well as the possible existence of a subsurface ocean.

In this paper, we present Juno UVS observations of Ganymede's aurora from both perijove (PJ) 34 and 35 flyby passes. The PJ34 flyby produced the highest spatial resolution observations of Ganymede's auroral emissions to date. We describe the observations in Section 2, results in Section 3, and end with our conclusions (Section 4).

2. Observations

On 7 June 2021, the Juno Ultraviolet Spectrograph (UVS) targeted Ganymede between 16:52 and 17:04 UTC. Juno UVS is an imaging ultraviolet spectrograph operating between 68 and 210 nm (Gladstone et al., 2017) with a 7.2° long slit. The slit is divided into three parts, two $2.55° \times 0.2°$ wide slits at the ends separated by a narrow $2.0° \times 0.025°$ slit in the middle (T. K. Greathouse et al., 2013). As Juno spun at 2 RPM (Bolton et al., 2017), UVS collected a scan across Ganymede every 30 s. We present the integrated 130.4 and 135.6 nm oxygen emissions measured by UVS through the two wide slits (Figure 1), as they exhibit the highest signal to noise (S/N) ratio. The data is mapped using the NAIF Spice toolkit (Acton, 1996) and the Juno Mission reconstructed kernels. Initial mapping produced a smoothly varying (in latitude and longitude) northern aurora, but the southern aurora surprisingly appeared to have a seemingly unphysical cusp or kink. After further analysis, it was found that a shift of −35 ms to the time of the retrieved UVS observations was needed to correctly map the auroral emissions to Ganymede (see Supporting Information S1). This temporal shift, a minor adjustment to the Juno spin phase, removed the apparent southern auroral kink and corrected the mapping of surface features observed by Juno's Stellar Reference Unit (SRU; Becker et al., 2022). Mapping the emissions to higher altitude enhanced the kink and required larger negative temporal shifts inconsistent with the SRU observations. This points to a near surface origin for the auroral emissions. Fortuitously, four views of the southern aurora were observed just off the limb of Ganymede (Figure 2). These observations show that the auroral emissions extend from the surface up to ∼25 km altitude (Figures 2b–2d) with a maximum extent of 50 km (Figure 2a).

The first spin of data which mapped to Ganymede's surface was retrieved at a nadir time (time of minimum UVS emission angle over a spin) of 16:53:25 UTC. This and the following four spins captured emissions from Ganymede's nightside while Juno's altitude decreased from 1,802 to 1,055 km. After that, the UVS scan mirror was moved from the extreme fore position to the extreme aft position (∼60° of motion) to retarget Ganymede, during which time no data was collected. The next spin captured data straddling the terminator at a nadir time of 16:57:55 UTC. The following 12 spins captured Ganymede's dayside at Juno altitudes from 1,827 to 7,779 km. These PJ34 data provide a sparse but high-resolution look at Ganymede's aurora with a best case nadir spatial resolution of 4 km (roughly 100× better than HST) degrading to 27 km for our last look upon departure.

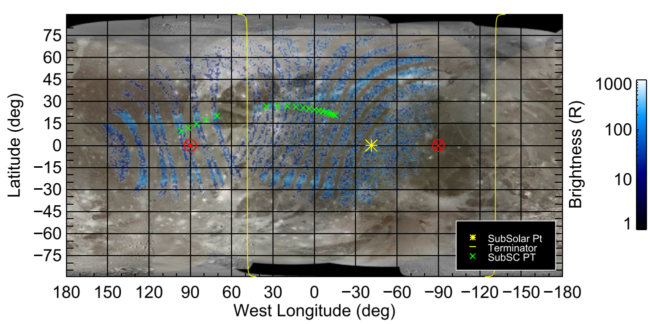

Figure 1. Brightness of the integrated 130.4 and 135.6 nm oxygen emissions observed during the Juno PJ34 Ganymede flyby, binned to a 1°-sampled cylindrical projection, scaled by cos(emission_angle), and overlaid on a USGS (Ganymede Voyager-Galileo SSI color global Mosaic 1.4 km v1) surface reflectance map. Green crosses note the sub-spacecraft position at the nadir time of each spin of collected data. The red symbols indicate the plasma flow direction.

10.1029/2022GL099794

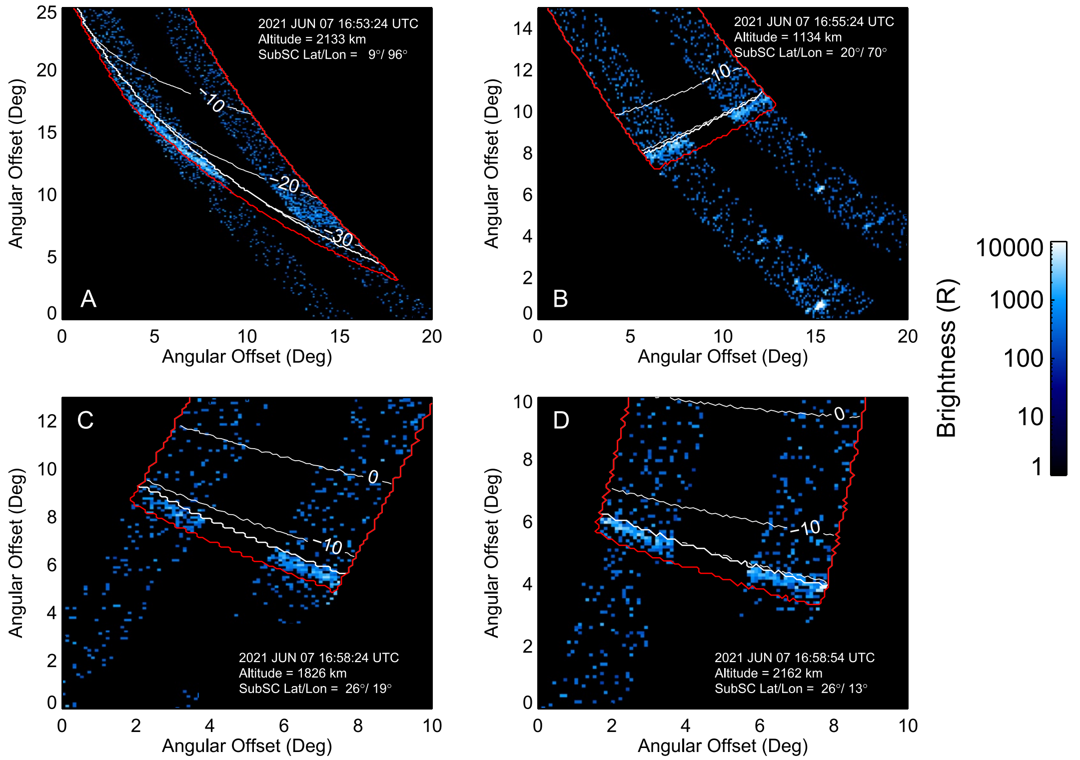

Figure 2. Integrated oxygen emission brightnesses as observed on sky show the vertical extent of auroral emissions at Ganymede. The white contours show the latitudes on Ganymede when mapping to the surface as well as the limb (southern most contour). The red contour traces the edges of the slit as well as the position of a 50 km altitude limb. The emissions all appear to extend from the surface up to an altitude of 25–50 km. Nadir times and sub-spacecraft altitudes, latitudes and west longitudes are given in each image.

On 20 July 2021, Juno made a second flyby of Ganymede on approach to PJ35. With a minimum Ganymede altitude of ∼50,000 km, the spatial resolution achieved by UVS (175 km best case) was by far worse than the previous flyby, but the greater distance meant UVS could target Ganymede for a much longer period of time, ∼1 hr. UVS captured data 16:32–16:48–17:27 UTC corresponding to altitudes of 52,610–50,109–67,060 km. The sum of all the PJ35 flyby data is shown in Figure S2 in Supporting Information S1 and Figure 6. Other geometric information is detailed in Hansen et al. (2022).

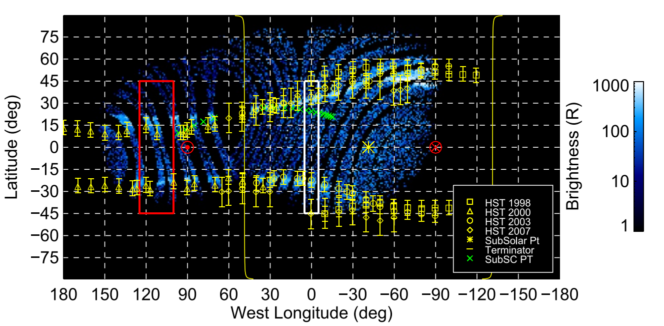

Figure 3. Integrated oxygen emission brightness, as in Figure 1, with the addition of the Hubble Space Telescope observations from McGrath et al. (2013) (see inset legend). The zonal average from the red box is shown in Figure 4a, and from the white box in Figure 4c.

3. Results

3.1. PJ34 Encounter

The PJ34 flyby of Ganymede offered the highest spatial-resolution observations of Ganymede's aurora to date. The position of the auroral emissions have previously been mapped using HST by McGrath et al. (2013). The mapping of these earlier observations are consistent with the UVS observations (Figure 3), while some variation of the position of the ovals is expected since models show their position depends on the plasma density in Jupiter's plasma disk (Duling et al., 2022) and the orientation of Jupiter's magnetic field (Saur et al., 2015), which are known to vary temporally. The brightness of the integrated oxygen lines corrected for emission angle (assuming optically thin emissions, consistent with Roth et al. (2021)) shows that the northern auroral oval on the trailing hemisphere is slightly brighter than the south (Figures 3 and 4c) suggesting the north may have been experiencing a slightly enhanced electron flux (see Section 3.2). To examine the variation of emission with latitude, we have taken the mean emission over longitude within two regions (red and white boxes) in Figure 3, plotting

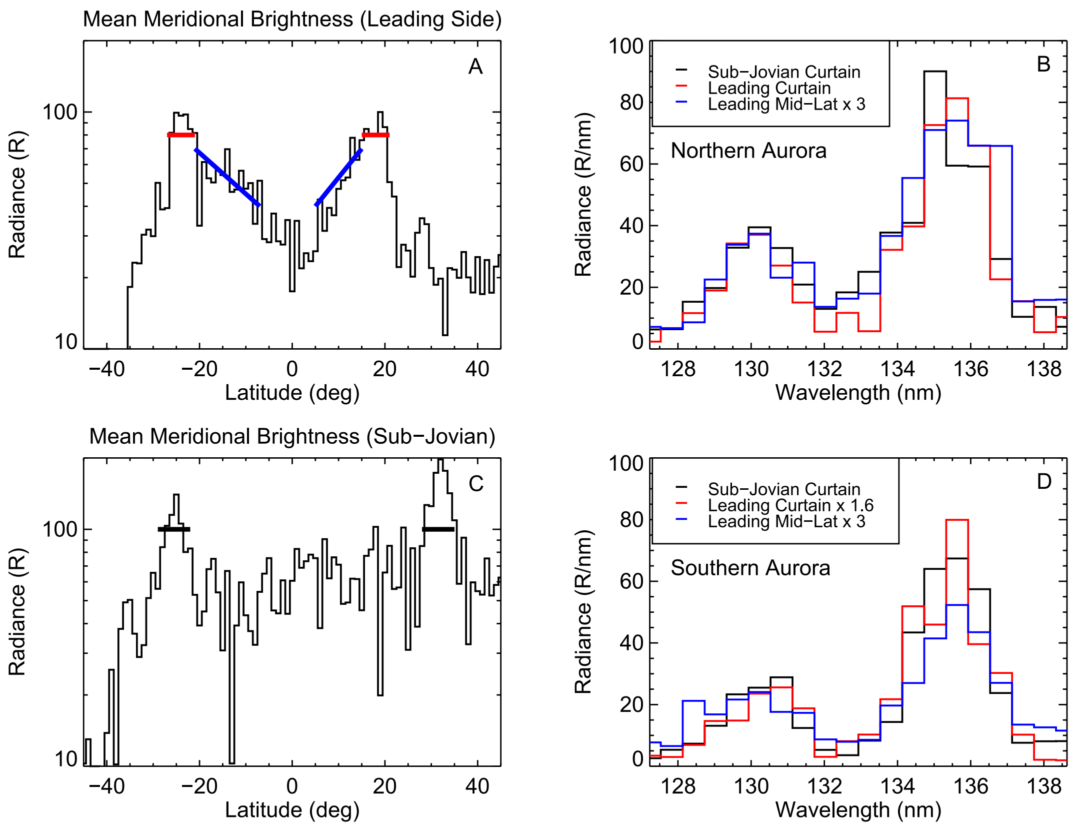

Figure 4. (a) Meridional average of the oxygen emissions within the red box (Figure 3) on the leading hemisphere and (c) within the white box centered on the sub-Jovian point (Figure 3). The spectral profile of the two oxygen lines for the northern aurora (b) and southern aurora (d) from the auroral curtain and leading-hemisphere lower-latitude emissions. Colored thick solid lines in panels (a and c) (red (−27°:−21°, 15°:21°), blue (−21°: −7°, 5°:15°), and black (−29°:−22°, 28°:35°)) correspond to latitudes extracted for the similarly colored spectra in panels (b and d).

the meridional trends in Figure 4a (red, leading hemisphere) and Figure 4c (white, sub-Jovian hemisphere). Both regions exhibit sharp polar boundaries to the auroral ovals with drops in intensity from on to off the aurora of factors of 3–4 (over 1°–2° of latitude). The auroras have a bright auroral curtain at the poleward boundary, approximately 3°–5° in latitude extent. The actual auroral curtain width may be somewhat narrower than this as there is some blurring in latitude in Figures 4a and 4c due to the latitude variation of the auroras with longitude and the need to average over longitude to increase our S/N. Interior to the auroral curtain (equatorward) on the leading hemisphere (Figure 4a), we see a drop in auroral emission by about a factor of 2 from the peak of the auroral curtain and then a slower decrease of emission from there toward the equator. Given the direction of the trend and the fact that these emissions are observed on the night side, this suggests there are precipitating electrons throughout most of the closed field line region on the leading hemisphere. The sub-Jovian (dayside) observations do not appear to exhibit this lower latitude emission trend. Looking at the oxygen emissions in more detail (Figures 4b and 4d), we find northern auroral oxygen 135.6/130.4 ratios of 1.8, 2.0, and 2.2 come from the sub-Jovian auroral curtain, leading-hemisphere auroral curtain, and leading-hemisphere mid-latitude emissions (Figure 4b), respectively. The southern auroral ratios are 2.3, 2.3, and 1.7 (Figure 4d), respectively. Since our S/N is rather low (requiring zonal binning to clearly see the emission trends) and it is clear the auroral curtain emissions on the dayside are an order of magnitude greater than the reflected sunlight emissions, we have not attempted to remove reflected sunlight from the dayside observations other than a spectral background subtraction from wavelengths on either side of the oxygen emissions. While Molyneux et al. (2018) found a disk averaged 135.6/130.4 ratio of 2.72 ± 0.57 on the leading hemisphere and a much lower value of 1.42 ± 0.16 for the trailing hemisphere, our results are more consistent with equal ratios for leading and trailing hemisphere auroral emissions of about 2. However, differences in the two studies such as geometry, sunlit versus nightside observations, a focus in this study on specifically the auroral regions and not disk averages, as well as extremely short integrations times by UVS (17 ms per spin) compared to almost half hour integrations from HST make comparing the results in the two studies complicated. For more detail about the dayside reflected emissions see Molyneux et al. (2018, 2022).

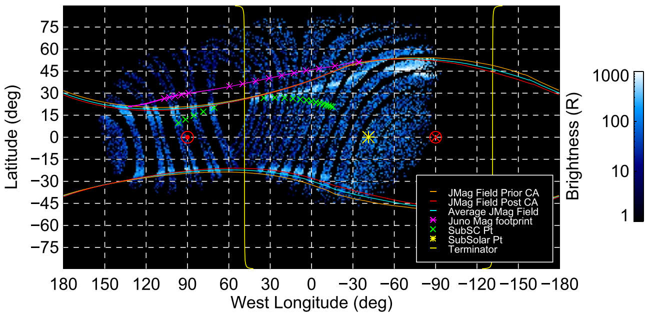

Figure 5. Same as Figure 3 with the addition of the mapping of the last-closed field-line boundaries using the Jovian magnetic field measured by the MAG instrument prior to, post, and interpolation of the two in orange, red, and cyan, respectively. The magenta line is the magnetic field-line tracing of the Juno spacecraft as modeled by Duling et al. (2022).

Detailed models (e.g., Duling et al., 2014; Jia et al., 2009; Saur et al., 2015) along with the results of Eviatar et al. (2001) suggest that the polar-most boundary of the auroral emissions is the position of the last closed field lines of Ganymede's magnetosphere. If this is indeed the case, then the Juno UVS observations provide a strong constraint on magnetospheric models, given that the PJ34 UVS data easily resolve this sharp polar boundary (see Figures 3 and 4). As an example, we compare the traces of the last-closed field-lines from the model of Duling et al. (2014), updated to the situation during Juno's flyby (Duling et al., 2022), to the UVS observations. Duling et al. (2022) used the Juno-measured magnetic field prior to closest approach, after closest approach, and then an interpolation of the two. The last-closed field-line boundary of those models are shown in Figures 5 and 6. In general, the model prediction of the position of the last-closed field-lines agree with the data very well. Only in the north between ±30° west longitude is there a maximum deviation, 8° of latitude, between the two. The prediction for the southern aurora is everywhere within 2° of latitude. One might think that the higher emission angle of the southern emission would make this boundary more difficult to measure, but given the small vertical extent of the emissions measured to be 25–50 km (Figure 2) compared to the much larger horizontal extent of the auroral curtains (3°–5° latitude equaling 140–230 km), this is not the case. Among several other upstream conditions and model parameters, the upstream thermal pressure affects the predicted position of the last-closed field-lines the most (Duling et al., 2022). Better knowledge of the upstream plasma conditions at encounter time and Ganymede's intrinsic field would likely improve the already good fit of the model to the observations.

One additional benefit of finding a field model that agrees with the observed auroral boundaries and in situ constraints of the Juno flyby data is that it allows accurate mapping of the magnetic footprint of the Juno spacecraft to the surface of Ganymede. This then allows for a direct connection to be made between in situ and remote sensing observations. We include the spacecraft magnetic field mapping to the surface of Ganymede derived from the Duling et al. (2022) model in Figure 5. From this model, it appears that Juno remained outside the closed-field line region during the PJ34 flyby (Allegrini et al., 2022; Clark et al., 2022; Duling et al., 2022) unfortunately not allowing a direct connection to be drawn from the in situ observations and auroral brightness observed by UVS.

3.2. PJ34 + PJ35

The combination of the PJ34 and PJ35 data set. allows for nearly complete longitudinal coverage of the auroras on Ganymede. The results display auroral emissions from both poles that are consistent with previous HST measurements and have the same general latitudinal variation as the model of Duling et al. (2022). For both flybys, Ganymede was located primarily south of the current sheet, magnetic latitude of −2.8° and −1.1° at the mid-point time of the PJ34 and PJ35 observations. In both cases, we find brighter northern auroral emissions than those in the south (Figures 4 and 6) in agreement with the Saur et al. (2022) finding that the brightness ratio of the northern and southern ovals oscillate with the oval closest to the current sheet center being the brightest.

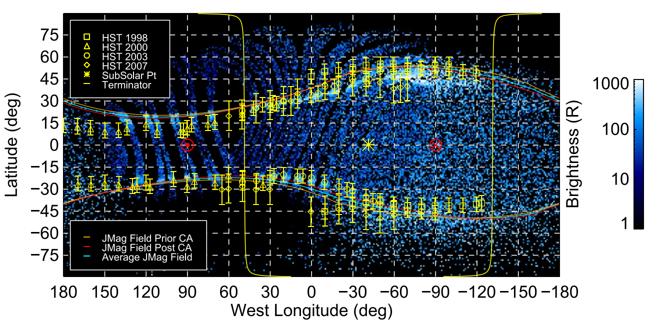

Figure 6. Brightness map of the integrated oxygen lines from both the PJ34 and PJ35 flyby data sets. Lines and symbols are the same as Figure 5.

4. Conclusions

The Juno mission's Ganymede close flyby positioned UVS to make unique observations of Ganymede's aurora emissions. We have discovered that Ganymede's auroral emissions originate from near the surface and extend 25–50 km in altitude. The enhanced spatial resolution relative to HST observations (i.e., McGrath et al., 2013) reveals that both ovals have a bright polar curtain about 5° in width, and the poleward-most edge has a steep dropoff in emission down to the background level of radiation noise within 1°–2° of latitude. On the leading hemisphere (night side) we detect lower intensity emissions from the equatorial side of the auroral curtain decreasing toward the equator. It is not yet clear what is driving these low-latitude emissions. Duling et al. (2022) modeling predicts last-closed field-line boundaries close to the observed auroral curtain positions except for a region between ±30° west longitude in the north. Future adjustments to modeled upstream plasma conditions may bring it into better agreement with the observations. Finally, it seems likely that Juno's trajectory passed just outside of Ganymede's closed field line region. This leaves some questions as to the energy and flux of particles related to the production of the observed UV emissions. Though Juno will not venture close to Ganymede again, the future is still bright with the coming of ESA's JUICE and NASA's Europa Clipper missions. Both missions carry similar UV instruments to Juno UVS which will enable even better observations of Ganymede's auroral emissions both spatially and temporally.

Data Availability Statement

The Juno data used in this study can be obtained from the Planetary Data System at https://pds-atmospheres.nmsu.edu/data_and_services/atmospheres_data/JUNO/uvs.html. Specifically, the calibrated data (Trantham, 2014) was used and combined into the Ganymede maps. The calibrated data is located at https://pds-atmospheres.nmsu.edu/cgi-bin/getdir.pl?dir=DATA%26volume=jnouvs_3001. All integrated maps/images used in the figures of the paper and Supporting Information S1 are archived (T. Greathouse et al., 2022) as idl save and FITS files.

Acknowledgments

This work was funded by the NASA's New Frontiers Program for Juno via contract NNM06AA75C with the Southwest Research Institute. B.B. is a Research Associate of the Fonds de la Recherche Scientifique—FNRS. S.D. and J.S. received funding from the European Research Council under the European Union's Horizon 2020 research and innovation program (Grant 884711). Special thanks to Melissa McGrath for supplying the HST data. The authors kindly thank the reviewers of this paper for their thoughtful reviews and comments.

References

Acton, C. H. (1996). Ancillary data services of NASA's navigation and ancillary information facility. *Planetary and Space Science*, *44*(1), 65–70. https://doi.org/10.1016/0032-0633(95)00107-7

Allegrini, F., Bagenal, F., Ebert, R. W., Louarn, P., McComas, D. J., Szalay, J. R., et al. (2022). Plasma observations during the 7 June 2021 Ganymede flyby from the Jovian Auroral Distributions Experiment (JADE) on Juno. *Geophysical Research Letters*, *49*, e2022GL098682. https://doi.org/10.1029/2022GL098682

Becker, H. N., Florence, M. M., Brennan, M. J., Hansen, C. J., Schenk, P. M., Ravine, M. A., et al. (2022). Surface features of Ganymede revealed in Jupiter-shine by Juno's Stellar Reference Unit. *Geophysical Research Letters*, *49*, e2022GL099139. https://doi.org/10.1029/2022GL099139

Bolton, S. J., Lunine, J., Stevenson, D., Connerney, J. E. P., Levin, S., Owen, T. C., et al. (2017). The Juno mission. *Space Science Reviews*, *213*(1), 5–37. https://doi.org/10.1007/s11214-017-0429-6

Clark, G., Kollmann, P., Mauk, B. H., Paranicas, C., Haggerty, D., Rymer, A., et al. (2022). Energetic charged particle observations during Juno's close flyby of Ganymede. *Geophysical Research Letters*, *49*, e2022GL099139. https://doi.org/10.1029/2022GL098572

Duling, S., Saur, J., Clark, G., Allegrini, F., Greathouse, T., Gladstone, R., et al. (2022). Ganymede MHD model: Magnetospheric context for Juno's PJ34 Flyby. https://doi.org/10.1002/essoar.10511409.1

Duling, S., Saur, J., & Wicht, J. (2014). Consistent boundary conditions at nonconducting surfaces of planetary bodies: Applications in a new Ganymede MHD model. *Journal of Geophysical Research: Space Physics*, *119*(6), 4412–4440. https://doi.org/10.1002/2013ja019554

Eviatar, A., Strobel, D. F., Wolven, B. C., Feldman, P. D., McGrath, M. A., & Williams, D. J. (2001). Excitation of the Ganymede ultraviolet aurora. *The Astrophysical Journal*, *555*(2), 1013–1019. https://doi.org/10.1086/321510

Feldman, P. D., McGrath, M. A., Strobel, D. F., Moos, H. W., Retherford, K. D., & Wolven, B. C. (2000). HST/STIS ultraviolet imaging of polar aurora on Ganymede. *The Astrophysical Journal*, *535*(2), 1085–1090. https://doi.org/10.1086/308889

Gladstone, G. R., Persyn, S. C., Eterno, J. S., Walther, B. C., Slater, D. C., Davis, M. W., et al. (2017). The ultraviolet spectrograph on NASA's Juno mission. *Space Science Reviews*, *213*(1–4), 447–473. https://doi.org/10.1007/s11214-014-0040-z

Greathouse, T., Gladstone, R., Molyneux, P., Versteeg, M., Hue, V., Kammer, J., et al. (2022). UVS observations of Ganymede's aurora during Juno orbits 34 and 35 (Mendeley Data, V1). https://doi.org/10.17632/6ghdtnsybz.1

Greathouse, T. K., Gladstone, G. R., Davis, M. W., Slater, D. C., Versteeg, M. H., Persson, K. B., et al. (2013). Performance results from in-flight commissioning of the Juno ultraviolet spectrograph (Juno-UVS). In *UV, X-ray, and gamma-ray space instrumentation for astronomy XVIII*, *8859*. https://doi.org/10.1117/12.2024537

Gurnett, D. A., Kurth, W. S., Roux, A., Bolton, S. J., & Kennel, C. F. (1996). Evidence for a magnetosphere at Ganymede from plasma-wave observations by the Galileo spacecraft. *Nature*, *384*(6609), 535–537. https://doi.org/10.1038/384535a0

Hall, D. T., Feldman, P. D., McGrath, M. A., & Strobel, D. F. (1998). The far-ultraviolet oxygen airglow of Europa and Ganymede. *The Astrophysical Journal*, *499*(1), 475–481. https://doi.org/10.1086/305604

Hansen, C. J., Bolton, S. J., Sulaiman, A. H., Duling, S., Bagenal, F., Brennan, M. J., et al. (2022). Juno's close encounter with Ganymede – An overview. *Geophysical Research Letters*, *49*, e2022GL099285. https://doi.org/10.1029/2022GL099285

Jia, X., Walker, R. J., Kivelson, M. G., Khurana, K. K., & Linker, J. A. (2009). Properties of Ganymede's magnetosphere inferred from improved three-dimensional MHD simulations. *Journal of Geophysical Research*, *114*(A9), A09209. https://doi.org/10.1029/2009ja014375

Kivelson, M. G., Khurana, K. K., Russell, C. T., Walker, R. J., Warnecke, J., Coroniti, F. V., et al. (1996). Discovery of Ganymede's magnetic field by the Galileo spacecraft. *Nature*, *384*(6609), 537–541. https://doi.org/10.1038/384537a0

McGrath, M. A., Jia, X., Retherford, K., Feldman, P. D., Strobel, D. F., & Saur, J. (2013). Aurora on Ganymede. *Journal of Geophysical Research: Space Physics*, *118*(5), 2043–2054. https://doi.org/10.1002/jgra.50122

Molyneux, P. M., Nichols, J. D., Bannister, N. P., Bunce, E. J., Clarke, J. T., Cowley, S. W. H., et al. (2018). Hubble Space Telescope observations of variations in Ganymede's oxygen atmosphere and aurora. *Journal of Geophysical Research: Space Physics*, *123*(5), 3777–3793. https://doi.org/10.1029/2018ja025243

Molyneux, P. M., Greathouse, T. K., Gladstone, G. R., Versteeg, M. H., Hue, V., Kammer, J., et al. (2022). Ganymede's UV reflectance from Juno-UVS data. *Geophysical Research Letters*, *49*, e2022GL099285. https://doi.org/10.1029/2022GL099285

Roth, L., Ivchenko, N., Gladstone, G. R., Saur, J., Grodent, D., Bonfond, B., et al. (2021). A sublimated water atmosphere on Ganymede detected from Hubble Space Telescope observations. *Nature Astronomy*, *5*(10), 1043–1051. https://doi.org/10.1038/s41550-021-01426-9

Saur, J., Duling, S., Roth, L., Jia, X., Strobel, D. F., Feldman, P. D., et al. (2015). The search for a subsurface ocean in Ganymede with Hubble Space Telescope observations of its auroral ovals. *Journal of Geophysical Research: Space Physics*, *120*(3), 1715–1737. https://doi.org/10.1002/2014ja020778

10.1029/2022GL099794

Saur, J., Duling, S., Wennmacher, A., Willmes, C., Roth, L., Strobel, D. F., et al. (2022). Alternating north-south brightness ratio of Ganymede's auroral ovals: Hubble Space Telescope observations around the Juno PJ34 flyby. *arXiv preprint arXiv:2208.09057*. https://doi.org/10.48550/arXiv.2208.09057

Trantham, B. (2014). *Juno Jupiter UVS Calibrated Data Archive V1.0*. PDS Atmospheres (ATM) Node. Retrieved from https://doi.org/10.17189/c32j-7r56